Journal of Molecular Liquids 277 (2019) 516–521

Contents lists available at ScienceDirect

Journal of Molecular Liquids

journal homepage: www.elsevier.com/locate/molliq

Ion flocculation in water: From bulk to nanoporous membrane desalination

Mateus H. Köhler [a,b,*], José R. Bordin [c], Marcia C. Barbosa [b]

[a] Departamento de Física, Universidade Federal de Santa Maria, 97105-900 Santa Maria, Brazil
[b] Instituto de Física, Universidade Federal do Rio Grande do Sul, 91501-970 Porto Alegre, Brazil
[c] Departamento de Física, Instituto de Física e Matemática, Universidade Federal de Pelotas, PO Box 354, 96010-900 Pelotas, Brazil

ARTICLE INFO

Article history:
Received 6 August 2018
Received in revised form 3 December 2018
Accepted 13 December 2018
Available online 18 December 2018

Keywords:
Desalination
Nanopores
Molybdenum disulfide
Graphene

ABSTRACT

In this work, we employed molecular dynamics simulations of a mixture of 1:1 and 3:1 salts in order to explore the flocculation as a prominent factor in desalination through nanoporous membranes. The NaCl rejection by the nanomembranes is enhanced due to the addition of the multivalent cation from ~70% to 100%. Our findings indicate that the mechanism behind this effect is the ionic clustering due to the presence of the multivalent ion combined with the dielectric discontinuity at the nanopore. We show that the confinement increases the sodium-sodium aggregation and that the clusters are able to support the high pressures applied in the non-equilibrium simulations. Our results indicate that a simple flocculant can enhance ion rejection rate of the nanomembrane, which is consistent with recent experimental findings that the rejection sharply increases with the particle size.

1. Introduction

The carbon nanotube (CNT) membranes with diameters smaller than 2 nm showed 100 to 1000 times higher permeability than existing polymeric membranes [1,2]. The mechanism behind this superflow is related to the favorable slip boundary condition found inside carbon nanostructures [3,4], which gives rise to several structural transitions in the confined water such as the single-file mobility found in small nanotubes [2,5]. Consequently, CNTs became an option for building membranes for desalination. However, the controlled production of nanotubes with diameter below 2 nm is not trivial and it is not obvious that the membrane of nanotubes resists to the high water pressures involved in the reverse osmosis desalination processes. Since the superflow of water observed in CNTs is not affected by the length of the tube [6], nano-sheet-based membranes [7–13] can be used instead of the CNT's as molecular sieving for water desalination. Two-dimensional (2D) nanoporous membranes have stood out in the last decade as prominent materials for cleaning water since they combine the unique molecular sieving properties with the fast permeation [14]. Recent advances in this field have allowed the introduction of 2D materials with tunable pore diameters and shapes [15–17], which are prerequisites for the industrial-scale production.

These materials, due to its single-atom thickness and mechanical robustness, became more attractive as membranes than structures such as conventional zeolite. As a consequence, several studies have focused on the chemical functionalization of the graphene nanopores [18–20]. For instance, Striolo and his group [21] has demonstrated that carboxyl functional groups tethered on graphene pores can enhance the ion exclusion, but the effect becomes less pronounced as both the ion concentration and the pore diameter increase. In addition, 2D materials with hydrophilic and hydrophobic sites, such as the molybdenum disulfide (MoS_2) nanopores, were investigated [13,22]. A nano-sheet of MoS_2 consists of a middle layer of molybdenum sandwiched between two sulfur layers, with thickness of ~1 nm and a robust Young's modulus of ~300 GPa [23] (comparable to the Young's modulus of steel).

The performance of current commercial reverse osmosis (RO) polymeric membranes is on the order of 0.1 $L/cm^2 \cdot day \cdot MPa$ (1.18 $g/m^2 \cdot s \cdot atm$) [24]. With the aid of zeolite nanosheets, permeability high as 1.3 $L/cm^2 \cdot day \cdot MPa$ can be obtained [25]. Recent studies have demonstrated that the MoS_2 nanopore filters can achieve very high water permeability of the order of 100 $g/m^2 \cdot s \cdot atm$ [22] — two orders of magnitude higher than the commercial RO based in polymeric membranes. This is comparable with the permeability measured experimentally for the graphene filter (~70 $g/m^2 \cdot s \cdot atm$) under similar conditions [26]. All of these results illustrate the high potential of 2D nanoporous membranes in desalination processes.

Although 2D membranes represent a huge step towards efficient water filtration, there are still experimental challenges concerning the nanopore tailoring. Some progress, however, has been made to produce

* Corresponding author at: Departamento de Física, Universidade Federal de Santa Maria, 97105-900 Santa Maria, Brazil.
E-mail address: mateuskohler@gmail.com (M.H. Köhler).

https://doi.org/10.1016/j.molliq.2018.12.077
0167-7322/

sub-nanometer controlled nanopores. Methods including electron beam [27], ion irradiation [28] and chemical etching [29] have been applied to introduce nanopores in graphene. Using a highly focused electron beam, and transmission electron microscope, versatile nanopores with diameters ranging from subnanometer to 10 nm were sculpted successfully in MoS_2 membranes [30]. Feng et al. [31] have developed a scalable method to controllably make nanopores in single-layer MoS_2 with subnanometer precision using electrochemical reaction (ECR). Fabrication of individual nanopores in hexagonal boron nitride (h-BN) with atomically precise control of the pore shape and size has been also reported [32]. Another challenge lies in accurately measuring the size of the manufactured nanopore. Attempts have been made to extract this information from the material's conductance [33]. Recently, Wen and colleagues [34] have introduced the concept of effective transport length in order to accurate determines graphene and MoS_2 nanopore's diameter using conductance measurements.

Despite the experimental efforts, the nanopores are often larger than the ion hydration radius. One way to get around this is to reduce the nanopore accessible area, but this lowers the water flux, which is not desirable. Another way to induce larger desalination rates is to increase the ionic cross section to avoid ion passage through the membrane. Joshi et al. [35] have reported experimental evidence that graphene oxide membranes can block all solutes with hydrated radii larger than ~0.45 nm. The ultrafast separation of small salts is attributed to an "ion sponge" effect that results in highly concentrated salt solutions inside graphene capillaries. Additionally, molecular dynamics (MD) simulations have confirmed that nanopores with ~1 nm in diameter allows the passage of monovalent ions but inhibits the passage of larger particles [35].

In this paper, we report a large increase in the salt rejection by graphene and MoS_2 membranes by promoting clusterization of the ions and increasing the ionic cross section. Instead of just pressing a NaCl solution against the nanomembrane, a flocculant ingredient, the ferric chloride ($Fe^{3+}Cl_3^-$), is added to the solution. The idea is to induce the monovalent ions to aggregate to the trivalent cation through a charge reversion mechanism [36,37]. Although in recent years a considerable amount of interest has been dedicated to the investigation of desalination processes using nanomembranes, to the best of our knowledge, the nanopore plus nano flocculant approach has not been investigated so far. We choose ferric chloride as flocculant once it is easily accessible, have a low cost, is an essential element for living organisms at low concentrations, and when at high concentrations can be easily removed from water.

2. Models and methods

We implemented MD simulations using the Large-scale Atomic/Molecular Massively Parallel Simulator (LAMMPS) package [38]. For the ion removal from water, two types of membranes are analyzed: MoS_2 and graphene. For analyzing the non-equilibrium flow the simulation box was built with a graphene sheet at one end acting as a rigid piston which applies an external force (pressure) on the ionic solution. The pressure gradient forces the solution against the 2D nanopore at the membrane located at the center of the box, as depicted in the Fig. 1 (a). The nanopore, with an accessible diameter of ~1 nm and illustrated in the Fig. 1(b), is located at the center of both the MoS_2 and the graphene sheets. The system contains 22,000 atoms distributed in a box with dimensions $5 \times 5 \times 13$ nm in x, y and z directions, respectively.

The ionic solution – pure sodium chloride or mixture of sodium and ferric chloride – has a total molarity of 1 M in all simulations. Although larger than the salinity of seawater (~0.6 M), it is in the same scale range and still reduces the computational cost associated with low-molarity solutions. We do not expect that this difference would change the behavior of the macroions. In order to study the effect of adding the ferric chloride to the NaCl solution, we investigate solutions with 20, 35 and 50% of Fe^{3+} ions.

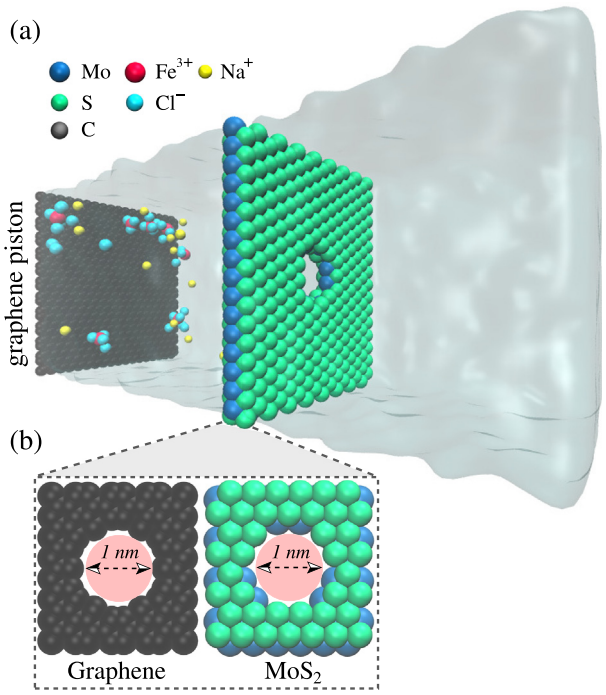

Fig. 1. (a) Schematic representation of the simulation framework. The system is divided as follows: On the left side we can see the piston (graphene) pressing the ionic solution (water, Fe^{3+}, Na^+, Cl^-) against the MoS_2 (or graphene) nanopore. On the right side we have bulk water. (b) Definition of the pore diameter for each membrane.

The TIP4P/2005 [39] water model was used and the SHAKE algorithm [40] was employed to maintain the rigidity of the water molecules. The non-bonded interactions are described by the Lennard-Jones (LJ) potential with a cutoff distance of 1 nm. The reader is referred to our previous work, reference [41], for more details about the parameters used in the simulations. The long-range electrostatic interactions were calculated by the *Particle Particle Particle Mesh* method [42] and periodic boundary conditions were applied in all directions.

For each non-equilibrium simulation with nanopore, the system was first equilibrated in the NPT ensemble for 10 ns at $P = 1$ atm and $T = 300$ K. Graphene and MoS_2 atoms were held fixed in the space during equilibration and the NPT simulations allow water to reach its equilibrium density (1 g/cm^3). After the pressure equilibration, a 10 ns simulation in the NVT ensemble was performed to further equilibrate the system at the same $T = 300$ K. Finally, a 10 ns production run were carried out, also in the NVT ensemble. Then different external pressures ($\Delta P = 10$, 50 and 100 MPa) were applied on the rigid piston to characterize the water filtration through the 2D (graphene and MoS_2) nanopores. We use such high pressures at MD simulations because low water flux would not go above the statistical error. The Nosé-Hoover thermostat [43,44] was used at each 0.1 ps in both NPT and NVT simulations, and the Nosé-Hoover barostat [45] was used to keep the pressure constant in the NPT simulations. For simplicity, the pores were held fixed in space to study solely the water transport and ion rejection properties of these materials. We carried out three independent simulations for each system collecting the trajectories of atoms every picosecond.

In order to assess whether the clusterization phenomenon is due to the confinement or rather an intrinsic behavior of the cations in solution we have further investigated the variation of Fe^{3+} concentration in equilibrium MD simulations for bulk or confined between two graphene sheets. The clusters properties were then compared with the non-equilibrium nanoporous simulation results. For the bulk and confined equilibrium systems, we have implemented 10 ns of NPT simulations followed by 30 ns of NVT simulations for data collection, in order to account for the equilibrium density of the ionic solution. The same

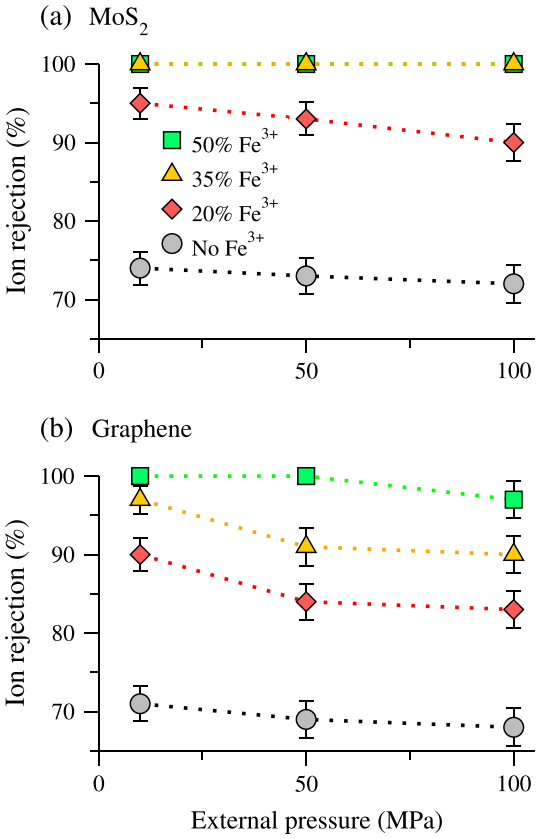

Fig. 2. Percentage of ion rejection as a function of the applied pressure for (a) MoS_2 and (b) graphene with distinct concentrations of ferric chloride. The dotted lines are a guide to the eye.

procedure was also adopted to simulate the *confined* systems. Again, we performed three independent simulations for each sample.

3. Results and discussion

The efficiency of a water desalination process is measured by the ability of the membrane to reject ions. The ion rejection depends on factors such as the nanopore's chemistry, size and shape, as well as the valence of the ion to be blocked [41]. Although the finite pore length has a minor effect in the water flow, it is quite relevant for the ionic structures [46]. The dielectric discontinuity – which has important consequences for the ion rejection – decreases as the length of the channel decreases and increases as the valence of the ion increases [47]. Therefore, the clusterization of ions in the solution leads to an increase of ion rejection both due to size and electrostatic effects.

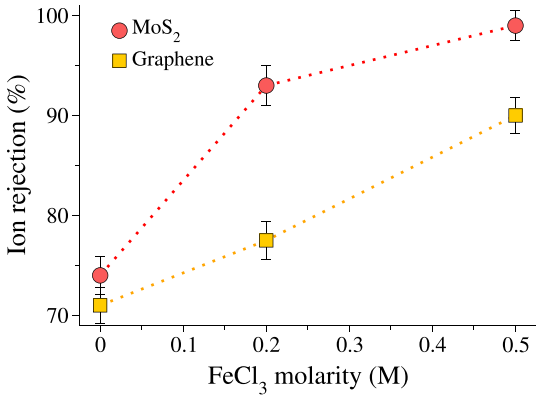

Fig. 4. Percentage of ion rejection as a function of the ferric chloride concentration (keeping NaCl molarity at 1 M) for MoS_2 and graphene nanopores under applied pressure $\Delta P = 10$ MPa.

3.1. Ionic rejection

The percentage of total ions rejected by the MoS_2 and graphene nanopores is plotted as a function of the applied pressure in Fig. 2. For low iron concentrations, Fig. 2(a) and (b) shows that the ion rejection decreases with the increase of pressure for both membranes. The higher pressures induce higher forces on the ions, allowing them to overcome the entropic and the dielectric barrier at the pore entrance. For higher iron concentrations, however, this is not the case. A complete ion rejection is observed for 35 and 50% of ferric chloride for the MoS_2 membrane and 50% of ferric chloride for the graphene membrane. The addition of ferric chloride increases the ion rejection by ~30% for the MoS_2 and ~32% for the graphene membranes when compared with the system without the flocculant. Additionally, the overall desalination is higher for the MoS_2 membrane compared with graphene, which is a consequence of the nozzle-like shape of the former and the

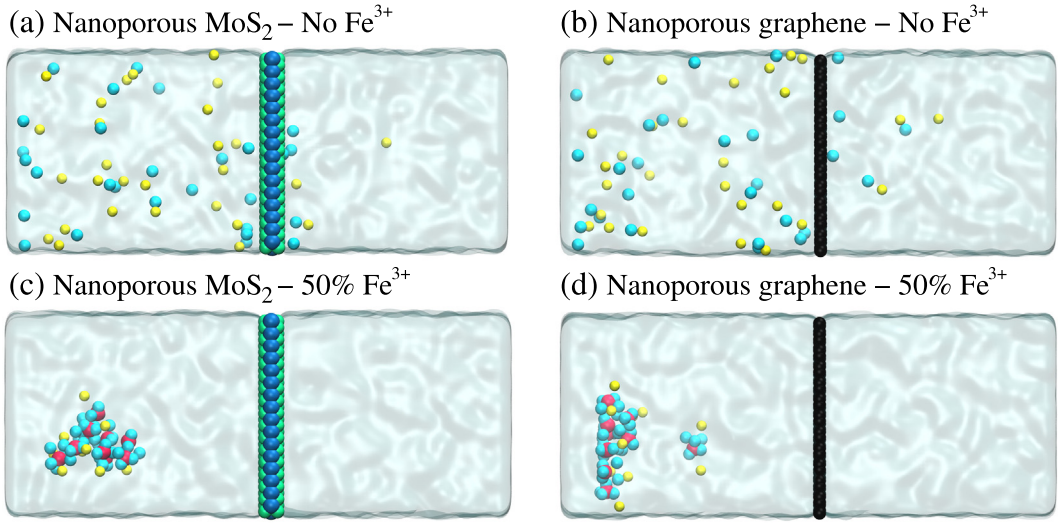

Fig. 3. (On the top) side view snapshots after 5 ns of simulations of NaCl passing through (a) MoS_2 and (b) graphene nanopore without any trace of clusterization. (Bottom) $FeCl_3$ cluster formation preventing the ion passage through (c) MoS_2 and (d) graphene nanopores. These configurations are for applied pressures of 50 MPa.

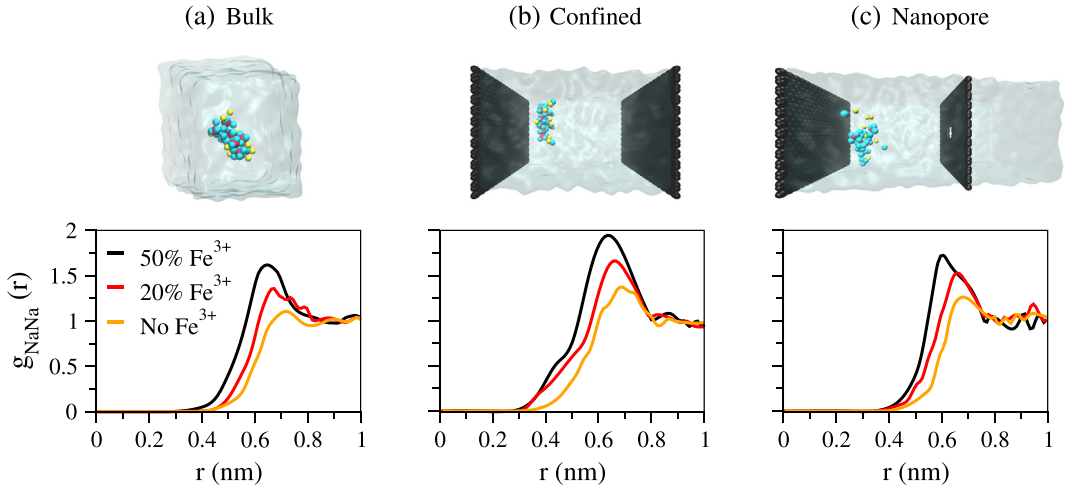

Fig. 5. Na—Na Radial distribution function for the ionic solution in (a) bulk, and confined between (a) graphene sheets and (c) nanoporous graphene. Different ferric chloride concentrations are considered.

hydrophilic-hydrophobic competition at the MoS_2 pore's edge [13]. In fact, the competition between hydrophilic and hydrophobic states is determinant for adhesion and blockage of ionic solutions in solid-liquid interfaces [48]. This would be useful, for instance, in nanopore power generators, with giant osmotic effects induced by ionic concentration bias [49].

The efficiency of desalination through nanoporous membranes is usually limited by the size of the pore: as the area of the pore increases, the efficiency of rejection decreases [13]. Here, we have used effective pore diameters (discounted the van der Waals radii) of ~1 nm, larger than that used by most of simulations with nanopores [13,22,50,51]. By adding ferric chloride to the solution we have achieved 100% of ion blockage, which is not observed in simple saline solutions even with functionalization of the nanopore [50,51]. The mechanism behind this new behavior is that adding $FeCl_3$ in the NaCl solution leads to the formation of ionic clusters. This clusterization is mainly regulated by the charge inversion phenomenon occurring when the Cl^- anions are attracted by Fe^{3+}, causing the excess of negative charge and the consequently inversion of sign in the charge distribution profile. Then, the Na^+ cation is attracted to this cluster. As result, the cross section of the clusters is larger than the accessible diameter of the pore. This phenomenon can be better observed in the snapshots depicted in Fig. 3. While in the absence of $FeCl_3$, Fig. 3(a) and (b), the ions spread out through the simulation box, when the ferric chloride is added to the solution the ions assemble to form big clusters, avoiding the ion passage through the membrane. The rejection is then mainly dictated by the size of these clusters: when we add enough Fe^{3+} to the system the cross section of the clusters becomes larger than the accessible area within the nanopore. Since the membrane rejection is most dependent on the ion/pore diameter ratio, with the addition of $FeCl_3$ we have highly increased the desalination efficiency of the nanopore.

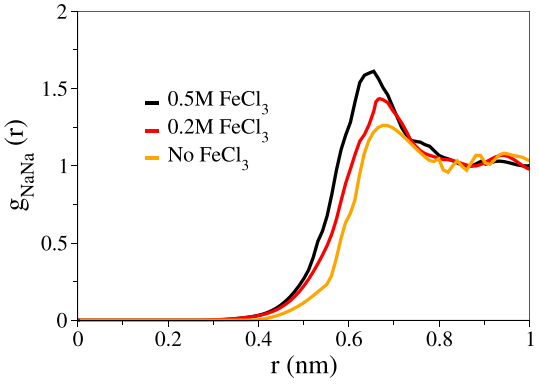

Fig. 6. Na—Na RDF for the ionic solution (1 M NaCl) in nanoporous graphene with different ferric chloride concentrations (0, 0.2 and 0.5 M $FeCl_3$).

In order to test whether the ionic rejection efficiency of the nanopore is due to the addition of the flocculant agent ($FeCl_3$) or due to the reduction of the NaCl molarity we have implemented simulations of 1 M NaCl solution with the addition of different amounts of ferric chloride (corresponding to 0, 0.2 and 0.5 M $FeCl_3$), thus increasing the total molarity of the solution. The ion rejection as a function of the ferric chloride molarity is shown in Fig. 4. We can observe that, as in the case of Fig. 2, the increase in the amount of $FeCl_3$ in the solution leads to an increase in the desalination rate. The difference is that while in the nanoporous graphene we observe a linear increase in the ion rejection until it reaches ~90%, the MoS_2 system is able to reject more than 90% of the ions by adding just 0.2 M of ferric chloride to the ionic solution. This result shows that regardless of keeping the overall solution molarity or adding the flocculant agent to a 1 M NaCl solution we observe a promising increase in the capability of the membrane to reject ions.

3.2. Ionic radial distribution and clustering

In order to understand if this clusterization is an artifact of the confinement or of the non-equilibrium nature of the flow we compared three cases: (i) bulk, (ii) confined between graphene sheets and (iii) the non-equilibrium nanopore case used for the water desalination simulations. Each case is represented in the insets of Fig. 5(a)–(c), respectively.

The Na—Na radial distribution functions (RDF) presented in Fig. 5 highlights the ionic clusterization process as we increase the Fe^{3+} concentration. For the bulk system, Fig. 5(a), we can observe that the sodium atoms become closer as the number of Fe^{3+} cations added to the solution increases. The same behavior is found for the other systems: regardless of the confinement (equilibrium graphene or non-equilibrium nanoporous graphene), the RDF shows the narrowing of Na—Na average distances as we increase the fraction of $FeCl_3$ in solution. The trend follows until the extreme situation in which we have 50% of ferric chloride, when we observe this highly packed ionic clusters both in bulk and in the confined solutions, as depicted in the insets of Fig. 5.

The fact that the ion clusters come through all the non-equilibrium simulations, with high applied pressures, is remarkable. In fact, solution neutron and X-ray diffraction have indicated that tri-valent ions do not significantly alter the density or orientation of water more than two water molecules (0.5 nm) away [52]. The short-range character of the ionic clusters in solution is therefore determinant for their survival

either in bulk or under applied pressures. This result is also corroborated by a recent investigation on the solvation of trivalent Al^{3+} both in bulk and confined between graphene sheets [53], where the trivalent cation do not significantly change the microstructure of the mixture. Despite the great interest on the structure and dynamics of ions in bulk water [54–57], very few experiments have been reported at the nanoscale confinement of ionic solutions. For the best of our knowledge, this is the first study reporting on the flocculation effect applied to water nanofiltration.

In Fig. 6 we show the Na—Na RDF for the 1 M NaCl solution without ferric chloride, and with the addition of 0.2 and 0.5 M $FeCl_3$. The curves show that independently of the NaCl to $FeCl_3$ ratio (if keeping the overall $FeCl_3$ + NaCl molarity at 1 M or keeping the 1 M NaCl solution with the addition of ferric chloride) we can observe the clustering of the Na atoms. The mechanism indicates again the flocculation capability of the $FeCl_3$, and therefore highlights the application of this ingredient in nanomembranes for efficient desalination.

All the results show that the ionic clusterization phenomenon is due to the ionic inversion effect associated with the addition of $FeCl_3$ to the solution. These clusters are then responsible for the increase in the ion rejection rate from a combination of size and repulsion due to the dielectric discontinuity. The flocculation represents therefore a potential method for improving desalination nanotechnologies.

4. Conclusions

Using molecular dynamics simulations we showed that adding ferric chloride to a salt water solution can significantly increase the salt rejection by the nanoporous membrane. Even for nanopores beyond 1 nm, where the efficiency of the membranes is low, the clustering process lead to a 100% salt rejection. Additionally, we have found a relation between the increase in ionic rejection and the percentage of $FeCl_3$ added to the NaCl solution. As we increase the proportion of ferric chloride the Na^+ ions aggregates forming large clusters, which is crucial for the ion blockage at the nanopore interface.

The flocculation phenomenon was found to be intrinsic of these ionic solutions (ferric chloride, sodium chloride and water) since we have observed large clusterization from the bulk phase to non-equilibrium confined systems. This result shows how we can improve the efficiency of nanoporous membranes for water desalination using flocculant chemicals.

Acknowledgements

This study was financed in part by the Coordenação de Aperfeiçoamento de Pessoal de Nível Superior (CAPES), Finance Code 001. The authors also acknowledge the Brazilian agencies CNPq, INCT-Fcx and FAPERGS for financial support, and CENAPAD-SP and CPAD-UFSM for the computer time. The authors thank Prof. Carolina de Matos and Prof. Jaqueline Vargas from UNIPAMPA for the inspirational discussions.

References

[1] J.K. Holt, H.G. Park, Y. Wang, M. Stadermann, A.B. Artyukhin, C.P. Grigoropoulos, A. Noy, O. Bakajin, Fast mass transport through sub-2-nanometer carbon nanotubes, Science 312 (2006) 1034.
[2] G. Hummer, J.C. Rasaiah, J.P. Noworyta, Water conduction through the hydrophobic channel of a carbon nanotube, Nature 414 (2001) 188.
[3] J.C.T. Eijkel, A. van den Berg, Nanofluidics: what is it and what can we expect from it? Microfluid. Nanofluid. 1 (2005) 249–267.
[4] R.S. Voronov, D.V. Papavassiliou, L.L. Lee, Review of fluid slip over superhydrophobic surfaces and its dependence on the contact angle, Ind. Eng. Chem. Res. 47 (2008).
[5] M.H. Köhler, J.R. Bordin, Surface, density, and temperature effects on the water diffusion and structure inside narrow nanotubes, J. Phys. Chem. C 122 (2018) 6684–6690.
[6] M.E. Suk, N.R. Aluru, Water transport through ultrathin graphene, J. Phys. Chem. Lett. 1 (2010) 1590–1594.
[7] Z. Li, Y. Qiu, K. Li, J. Sha, T. Li, Y. Chen, Optimal design of graphene nanopores for seawater desalination, J. Chem. Phys. 148 (2018) 014703.
[8] J. Azamat, A. Khataee, F. Sadikoglu, Computational study on the efficiency of MoS_2 membrane for removing arsenic from contaminated water, J. Mol. Liq. 249 (2018) 110–116.
[9] B. Chen, H. Jiang, X. Liu, X. Hu, Observation and analysis of water transport through graphene oxide interlamination, J. Phys. Chem. C 121 (2017) 1321–1328.
[10] M. Dahanayaka, B. Liu, Z. Hu, Q.-X. Pei, Z. Chen, A.W.-K. Law, K. Zhou, Graphene membranes with nanoslits for seawater desalination via forward osmosis, Phys. Chem. Chem. Phys. 19 (2017) 30551–30561.
[11] H. Gao, Q. Shi, D. Rao, Y. Zhang, J. Su, Y. Liu, Y. Wang, K. Deng, R. Lu, Rational design and strain engineering of nanoporous boron nitride nanosheet membranes for water desalination, J. Phys. Chem. C 121 (2017) 22105–22113.
[12] J. Kou, J. Yao, L. Wu, X. Zhou, H. Lu, F. Wu, J. Fan, Nanoporous two-dimensional MoS_2 membranes for fast saline solution purification, Phys. Chem. Chem. Phys. 18 (2016) 22210–22216.
[13] M. Heiranian, A.B. Farimani, N.R. Aluru, Water desalination with a single-layer MoS_2 nanopore, Nat. Commun. 6 (2015) 8616.
[14] G. Xu, J. Xu, H. Su, X. Liu, Lu-Li, H. Zhao, H. Feng, R. Das, Two-dimensional (2D) nanoporous membranes with sub-nanopores in reverse osmosis desalination: latest developments and future directions, Desalination 451 (2019) 18–34.
[15] K. Liu, M. Lihter, A. Sarathy, S. Caneva, H. Qiu, D. Deiana, V. Tileli, D.T.L. Alexander, S. Hofmann, D. Dumcenco, A. Kis, J.-P. Leburton, A. Radenovic, Geometrical effect in 2D nanopores, Nano Lett. 17 (2017) 4223–4230.
[16] B. Chen, H. Jiang, X. Liu, X. Hu, Molecular insight into water desalination across multilayer graphene oxide membranes, ACS Appl. Mater. Interfaces 9 (2017) 22826–22836.
[17] B. Chen, H. Jiang, X. Liu, X. Hu, Water transport confined in graphene oxide channels through the rarefied effect, Phys. Chem. Chem. Phys. 20 (2018) 9780–9786.
[18] V. Georgakilas, M. Otyepka, A.B. Bourlinos, V. Chandra, N. Kim, K.C. Kemp, P. Hobza, R. Zboril, K.S. Kim, Functionalization of graphene: covalent and non-covalent approaches, derivatives and applications, Chem. Rev. 112 (2012) 6156–6214.
[19] K.A. Mahmoud, B. Mansoor, A. Mansour, M. Khraisheh, Functional graphene nanosheets: the next generation membranes for water desalination, Desalination 356 (2015) 208–225.
[20] Z. Hu, B. Liu, M. Dahanayaka, A.W.-K. Law, J. Wei, K. Zhou, Ultrafast permeation of seawater pervaporation using single-layered C_2N via strain engineering, Phys. Chem. Chem. Phys. 19 (2017) 15973–15979.
[21] D. Konatham, J. Yu, T.A. Ho, A. Striolo, Simulation insights for graphene-based water desalination membranes, Langmuir 29 (2013) 11884–11897.
[22] W. Li, Y. Yang, J.K. Weber, G. Zhang, R. Zhou, Tunable, strain-controlled nanoporous MoS_2 filter for water desalination, ACS Nano 10 (2016) 1829–1835.
[23] S. Bertolazzi, J. Brivio, A. Kis, Stretching and breaking of ultrathin MoS_2, ACS Nano 5 (2011) 9703–9709.
[24] M.T.M. Pendergast, E.M.V. Hoek, A review of water treatment membrane nanotechnologies, Energy Environ. Sci. 4 (2011) 1946–1971.
[25] S.H. Jamali, T.J.H. Vlugt, L.-C. Lin, Atomistic understanding of zeolite nanosheets for water desalination, J. Phys. Chem. C 121 (2017) 11273–11280.
[26] S.P. Surwade, S.N. Smirnov, I.V. Vlassiouk, R.R. Unocic, G.M. Veith, S. Dai, S.M. Mahurin, Water desalination using nanoporous single-layer graphene, Nat. Nanotechnol. 10 (2015) 459–464.
[27] S. Garaj, W. Hubbard, A. Reina, J. Kong, D. Branton, J.A. Golovchenko, Graphene as a subnanometre trans-electrode membrane, Nature 467 (2010) 190–193.
[28] K. Yoon, A. Rahnamoun, J.L. Swett, V. Iberi, D.A. Cullen, I.V. Vlassiouk, A. Belianinov, S. Jesse, X. Sang, O.S. Ovchinnikova, A.J. Rondinone, R.R. Unocic, A.C.T. van Duin, Atomistic-scale simulations of defect formation in graphene under noble gas ion irradiation, ACS Nano 10 (2016) 8376–8384.
[29] S.C. Ohern, D. Jang, S. Bose, J.-C. Idrobo, Y. Song, T. Laoui, J. Kong, R. Karnik, Nanofiltration across defect-sealed nanoporous monolayer graphene, Nano Lett. 15 (2015) 3254–3260.
[30] K. Liu, J. Feng, A. Kis, A. Radenovic, Atomically thin molybdenum disulfide nanopores with high sensitivity for DNA translocation, ACS Nano 8 (2014) 2504–2511.
[31] J. Feng, K. Liu, M. Graf, M. Lihter, R.D. Bulushev, D. Dumcenco, D.T.L. Alexander, D. Krasnozhon, T. Vuletic, A. Kis, A. Radenovic, Electrochemical reaction in single layer MoS_2: nanopores opened atom by atom, Nano Lett. 15 (2015) 3431–3438.
[32] S.M. Gilbert, G. Dunn, A. Azizi, T. Pham, B. Shevitski, E. Dimitrov, S. Liu, A. Shaul, A. Zettl, Fabrication of subnanometer precision nanopores in hexagonal boron nitride, Sci. Rep. 7 (2017) 15096.
[33] C.M. Frament, J.R. Dwyer, Conductance-based determination of solid-state nanopore size and shape: an exploration of performance limits, J. Phys. Chem. C 116 (2012) 23315–23321.
[34] C. Wen, Z. Zhang, S.-L. Zhang, Physical model for rapid and accurate determination of nanopore size via conductance measurement, ACS Sens. 2 (2017) 1523–1530.
[35] R.K. Joshi, P. Carbone, F.C. Wang, V.G. Kravets, Y. Su, I.V. Grigorieva, H.A. Wu, A.K. Geim, R.R. Nair, Precise and ultrafast molecular sieving through graphene oxide membranes, Science 343 (2014) 752–754.
[36] S. Pianegonda, M.C. Barbosa, Y. Levin, Charge reversal of colloidal particles, Europhys. Lett. 71 (2005) 831–837.
[37] A. Diehl, Y. Levin, Colloidal charge reversal: dependence on the ionic size and the electrolyte concentration, J. Chem. Phys. 129 (2008) 124506.
[38] S. Plimpton, Fast parallel algorithms for short-range molecular dynamics, J. Comput. Phys. 117 (1995) 1–19.
[39] J. Abascal, C. Vega, A general purpose model for the condensed phases of water: TIP4P/2005, J. Chem. Phys. 123 (2005) 234505.
[40] J.-P. Ryckaert, G. Ciccotti, H.J.C. Berendsen, Numerical integration of the Cartesian equations of motion of a system with constraints: molecular dynamics of n-alkanes, J. Comput. Phys. 23 (1977) 327–341.

[41] M.H. Köhler, J.R. Bordin, M.C. Barbosa, 2D nanoporous membrane for cation removal from water: effects of ionic valence, membrane hydrophobicity, and pore size, J. Chem. Phys. 148 (2018) 222804.
[42] R.W. Hockney, J.W. Eastwood, Computer Simulation Using Particles, McGraw-Hill, New York, 1981.
[43] S. Nosé, A molecular dynamics method for simulation in the canonical ensemble, Mol. Phys. 52 (1984) 255.
[44] W.G. Hoover, Canonical dynamics: equilibrium phase-space distributions, Phys. Rev. A 31 (1985) 1695.
[45] G.J. Martyna, D.J. Tobias, M.L. Klein, Constant pressure molecular dynamics algorithms, J. Chem. Phys. 101 (5) (1994) 4177–4189.
[46] K. Breitsprecher, M. Abele, S. Kondrat, C. Holm, The effect of finite pore length on ion structure and charging, J. Chem. Phys. 147 (2017) 104708.
[47] J.R. Bordin, A. Diehl, M.C. Barbosa, Y. Levin, Ion fluxes through nanopores and transmembrane channels, Phys. Rev. E 85 (2012) 031914.
[48] D. Surblys, F. Leroy, Y. Yamaguchi, F. Muller-Plathe, Molecular dynamics analysis of the influence of Coulomb and van der Waals interactions on the work of adhesion at the solid-liquid interface, J. Chem. Phys. 148 (2018) 134707.
[49] Z. Huang, Y. Zhang, T. Hayashida, Z. Ji, Y. He, M. Tsutsui, X.S. Miao, M. Taniguchi, The impact of membrane surface charges on the ion transport in MoS_2 nanopore power generators, Appl. Phys. Lett. 111 (2017) 263104.
[50] D. Cohen-Tanugi, J.C. Grossman, Water desalination across nanoporous graphene, Nano Lett. 12 (2012) 3602–3608.
[51] D. Cohen-Tanugi, L.-C. Lin, J.C. Grossman, Multilayer nanoporous graphene membranes for water desalination, Nano Lett. 16 (2016) 1027–1033.
[52] Kim D. Collins, George W. Neilson, John E. Enderby, Ions in water: characterizing the forces that control chemical processes and biological structure, Biophys. Chem. 128 (2007) 95–104.
[53] V. Gómez-González, B. Docampo-Alvarez, H. Montes-Campos, J.C. Otero, E.L. Lago, O. Cabeza, L.J. Gallego, L.M. Varela, Solvation of Al^{3+} cations in bulk and confined protic ionic liquids: a computational study, Phys. Chem. Chem. Phys. 20 (2018) 19071–19081.
[54] M.D. Boamah, P.E. Ohno, F.M. Geiger, K.B. Eisenthal, Relative permittivity in the electrical double layer from nonlinear optics, J. Chem. Phys. 148 (2018) 222808.
[55] J.A. Devine, A. Abou Taka, M.C. Babin, M.L. Weichman, H.P. Hratchian, D.M. Neumark, High-resolution photoelectron spectroscopy of $TiO_3H_2^-$: probing the $TiO_2^- + H_2O$ dissociative adduct, J. Chem. Phys. 148 (2018) 222810.
[56] I. Waluyo, D. Nordlund, U. Bergmann, D. Schlesinger, L.G.M. Pettersson, A. Nilsson, A different view of structure-making and structure-breaking in alkali halide aqueous solutions through X-ray absorption spectroscopy, J. Chem. Phys. 140 (2014) 244506.
[57] P. Ben Ishai, E. Mamontov, J.D. Nickels, A.P. Sokolov, Influence of ions on water diffusion — a neutron scattering study, J. Phys. Chem. B 117 (2013) 7724–7728.